

Rotational spectroscopy of oxirane-2,2- d_2 , c - $\text{CD}_2\text{CH}_2\text{O}$, and its tentative detection toward IRAS 16293–2422 B

Holger S.P. Müller^{a,*}, Jes K. Jørgensen^b, Jean-Claude Guillemin^c, Frank Lewen^a, Stephan Schlemmer^a

^a*Astrophysik/I. Physikalisches Institut, Universität zu Köln, Zùlpicher Str. 77, 50937 Köln, Germany*

^b*Niels Bohr Institute, University of Copenhagen, Øster Voldgade 5–7, 1350 Copenhagen K, Denmark*

^c*Univ Rennes, Ecole Nationale Supérieure de Chimie de Rennes, CNRS, ISCR–UMR 6226, 35000 Rennes, France*

Abstract

We prepared a sample of oxirane doubly deuterated at one C atom and studied its rotational spectrum in the laboratory for the first time between 120 GHz and 1094 GHz. Accurate spectroscopic parameters up to eighth order were determined, and the calculated rest frequencies were used to identify c - $\text{CD}_2\text{CH}_2\text{O}$ tentatively in the interstellar medium in the Atacama Large Millimeter/submillimeter Array Protostellar Interferometric Line Survey (PILS) of the Class 0 protostellar system IRAS 16293–2422. The c - $\text{CD}_2\text{CH}_2\text{O}$ to c - $\text{C}_2\text{H}_4\text{O}$ ratio was estimated to be ~ 0.054 with $T_{\text{rot}} = 125$ K. This value translates to a D-to-H ratio of ~ 0.16 per H atom which is higher by a factor of 4.5 than the ~ 0.036 per H atom obtained for c - $\text{C}_2\text{H}_3\text{DO}$. Such increase in the degree of deuteration referenced to one H atom in multiply deuterated isotopologs compared to their singly deuterated variants have been observed commonly in recent years.

Keywords:

rotational spectroscopy, submillimeter spectroscopy, interstellar molecule, molecular symmetry, reduced Hamiltonian

1. Introduction

Oxirane, c - $\text{C}_2\text{H}_4\text{O}$, is a small cyclic molecule that is also known as ethylene oxide, oxacyclopropane, epoxyethane, and dimethylene oxide. Here and in the following, unlabeled C and O atoms refer to ^{12}C and ^{16}O , respectively. The molecule was detected in a multitude of astronomical sources such as high- and low-mass star-forming regions and prestellar cores [1, 2, 3, 4, 5, 6]. Its rotational spectrum was recorded in the early days of microwave spectroscopy and include the determination of structural parameters and of its dipole moment through Stark effect measurements [7]. Several further investigations were carried out for the main isotopolog since then [8, 9, 10, 11]. The spectra of numerous isotopic species, including multiply substituted ones, were also recorded [12, 13], albeit in the microwave and lower millimeter-wave regions only until quite recently. A sample in natural isotopic composition was used to extend the c - $^{13}\text{CCH}_4\text{O}$ and c - $\text{C}_2\text{H}_4^{18}\text{O}$

data sets into the upper millimeter and submillimeter regions [11]. In addition, isotopically enriched samples were employed to investigate the rotational spectrum of mono-deuterated oxirane, c - $\text{C}_2\text{H}_3\text{DO}$, in the millimeter and far-infrared regions [14] and in the submillimeter region [15]. The combined data of these two studies and an earlier one [12] led to the detection of c - $\text{C}_2\text{H}_3\text{DO}$ toward IRAS 16293–2422 [15].

IRAS 16293–2422 is a Class 0 solar-type protostellar system and an astrochemical template source. The results on c - $\text{C}_2\text{H}_3\text{DO}$ were obtained in the framework of the Protostellar Interferometric Line Survey (PILS), which is an unbiased molecular line survey of this source around 345 GHz carried out with the Atacama Large Millimeter/submillimeter Array (ALMA) to study its physical conditions and molecular complexity [16]. Among the most prominent results of PILS were the detections of the organohalogen compound methyl chloride (CH_3Cl) [17], nitrous acid (HONO) [18], and the tentative detection of 3-hydroxypropenal [19]. Several other molecules were detected for the first time in a low-mass star-forming region in the PILS data, among them oxirane, propanal, and propanone [5], the

*Corresponding author.

Email address: hspm@ph1.uni-koeln.de (Holger S.P. Müller)

latter is also known as acetone. Noteworthy are also the first interstellar detections of a plethora of isotopic species containing, in particular, ^{13}C or D. Several examples and an overview of the detections at that time were given in [20]; more recent examples were summarized in [15].

The enrichment of deuterium in dense molecular clouds has attracted considerable interest for many years, as it has been viewed as an evolutionary tracer in low-mass star-forming regions and/or a means to trace the formation histories of complex organic molecules [21, 22, 23, 24, 25]. An important aspect in this context is the observation that the degree of deuteration referenced to one H atom is frequently higher in multiply deuterated isotopologs than in the mono-deuterated isotopologs. Examples from PILS are D_2CO [26], CHD_2CN [27], CHD_2OCHO [28], CHD_2OCH_3 [29], CHD_2OH [30], and CD_3OH [31]. Other examples include D_2S [32], HD_2^+ [33], ND_2 [34] and D_2O [35]. The higher degree of deuteration per H atom for multiply deuterated isotopologs compared with the respective singly deuterated ones was proposed to be inherited from the prestellar phase. An investigation into the deuteration of thioformaldehyde of the prestellar core L1544 [36] supports this proposal. Additional support comes from laboratory studies of the D-to-H and H-to-D exchange of formaldehyde isotopologs at very low temperatures where the first reaction proceeds faster than the second and leads to more D_2CO than expected from a statistical distribution of D between H_2CO , HDCO , and D_2CO [37]. The degree of deuteration in $c\text{-C}_2\text{H}_3\text{DO}$ and its line intensities were sufficiently high in the PILS data that it appeared plausible to detect doubly deuterated oxirane as well [15]. While there is only one singly deuterated oxirane isotopomer, there are three in the case of doubly deuterated oxirane: oxirane-2,2- d_2 , oxirane-*anti*-2,3- d_2 , and oxirane-*syn*-2,3- d_2 . An early, limited microwave study of the last two isotopomers [12] has been extended recently [38], but has not appeared in the literature yet to the best of our knowledge. No rotational data have been published for the isotopomer oxirane-2,2- d_2 . Therefore, we decided to synthesize it, analyze its rotational spectrum, and search for it in the PILS data.

2. Laboratory spectroscopic details

Our measurements were carried out at room temperature using two different spectrometers. Pyrex glass cells with an inner diameter of 100 mm were used in both cases. Both employ VDI frequency multipliers driven

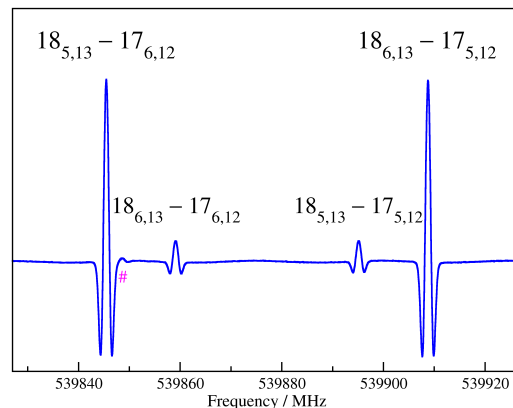


Figure 1: Section of the rotational spectrum of $c\text{-CD}_2\text{CH}_2\text{O}$. Two stronger b -type transitions approach oblate pairing and are accompanied by weaker a -type transitions between them. The weak line indicated by the magenta pound sign is the $12_{10,5} - 14_{10,4}$ transition of $c\text{-C}_2\text{H}_3\text{DO}$ which is present as an impurity.

by Rohde & Schwarz SMF 100A microwave synthesizers as sources. A Schottky diode detector was employed between 120 and 181 GHz, a closed cycle liquid He-cooled InSb bolometer (QMC Instruments Ltd) was utilized between 490 and 1094 GHz. We applied frequency modulation throughout to reduce baseline affects. The demodulation at $2f$ causes an isolated line to appear close to a second derivative of a Gaussian, as is displayed in Fig. 1.

Two connected 7 m long double pass cells equipped with Teflon lenses were utilized for measurements between 120 and 181 GHz. The pressures were between 1.0 and 1.5 Pa. Further information on this spectrometer is available elsewhere [39]. Measurements between 490 and 1094 GHz were performed using a 5 m long single pass cell at pressures of ~ 0.5 Pa to around 3 Pa. Further information on this spectrometer system is available in [40].

The 490–750 GHz region was recorded in its entirety one time at a pressure of 1.0 Pa and lower detector sensitivity to avoid saturation effects on the strongest lines. The spectral region was recorded a second time at a pressure of 3.0 Pa with higher detector sensitivity and slightly higher modulation depth to optimize the signal-to-noise ratio (S/N) for weak lines. The assigned line uncertainties were dominated by the line shape; the S/N was important in particular for weaker symmetric lines. We assigned 5 kHz to strong, isolated, and very symmetric lines up to 50 kHz for weak and somewhat asymmetric lines or lines fairly close to other lines. This is in keeping with our investigations on $c\text{-C}_2\text{H}_4\text{O}$ [11]

and c -C₂H₃DO [15]. Frequency accuracies of 10 kHz were achieved at even higher frequencies for H₂C¹⁸O and H₂C¹⁷O measured in natural isotopic composition [41] as well as for excited vibrational states of CH₃CN [42].

Individual transitions were recorded in the other frequency windows. Strong and very strong lines were recorded between 973 and 1094 GHz at pressures of 1.0 and ~0.5 Pa, respectively. The very high S/N and the very symmetric line shapes yielded uncertainties of 3 and 2 kHz, respectively. Weak lines with high K_a and very weak lines with high K_c were recorded between 765 and 963 GHz at a pressure of 3 Pa. The accuracies are between 10 and 50 kHz.

Finally, several stronger and some weaker transitions were recorded between 120 and 181 GHz. We achieved frequency accuracies of 5 kHz for the best lines for this spectrometer system in a study of 2-cyanobutane [43] which is a molecule with a much richer rotational spectrum. The S/N was very good for all lines in the present case such that the line uncertainties appeared to depend solely on the line shapes. They are between 2 kHz for very symmetric lines to 10 or 15 kHz for less symmetric lines.

3. Synthesis of doubly deuterated oxirane, c -CD₂CH₂O

3.1. 2-Chloroethanol-1,1- d_2

Sodium borodeuteride (98 atom % D, 1.0 g, 24 mmol) and dry tetrahydrofuran (THF) (10 mL) were introduced under nitrogen into a three-necked flask. Dry chloroacetic acid (2.26 g, 24 mmol) in dry THF (10 mL) was added dropwise and evolution of hydrogen gas was observed. The reaction mixture was refluxed for 6 h, cooled to room temperature and then hydrolyzed with 3 N-D₂SO₄, made alkaline with aqueous sodium carbonate, extracted with diethyl ether, and dried over MgSO₄. The solvent was carefully removed under vacuum and the purification was carried out on a vacuum line (0.1 mbar) with a trap cooled to -60°C to selectively trap the 2-chloroethanol-1,1- d_2 . Two distillations gave 1.2 g pure product (60% yield) with an isotopic purity of about 90%.

¹H NMR (CDCl₃, 400 MHz) δ 3.09 (s, brd, 1H, OH), 3.60 (s, 2H, CH₂Cl). ¹³C NMR (CDCl₃, 100 MHz) δ 46.2 (¹J_{CH} = 149.9 Hz (t), CH₂Cl), 62.0 (¹J_{CD} = 22.0 Hz (quint.), CD₂).

3.2. Oxirane-2,2- d_2

2-Chloroethanol-1,1- d_2 (1.0 g, 14.4 mmol) was vaporized in a vacuum line (0.1 mbar) on *t*-BuOK in pow-

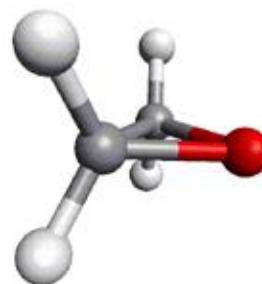


Figure 2: Model of the c -C₂H₄O molecule. The C atoms are shown in gray, the H atoms in light gray and the O atom in red. The O atom and the mid-point of the CC bond are on the b -axis. The two D atoms in c -CD₂CH₂O are attached to the same C atom, causing a slight rotation of its inertial axis system in the ab - (or COC) plane compared with c -C₂H₄O which leads to a small a -dipole moment component.

der which was heated to 90°C; similar experiments are described in greater detail elsewhere [44]. A trap cooled to -100°C removed selectively the impurities (mainly *t*-butanol), and oxirane-2,2- d_2 was selectively condensed in a trap cooled at 77 K. The yield was 0.38 g or 67%.

¹H NMR (CDCl₃, 400 MHz) δ 2.60 (m, 2H, CH₂). ¹³C NMR (CDCl₃, 100 MHz) δ 40.0 (¹J_{CD} = 26.9 Hz (quint.), CD₂), 40.5 (¹J_{CH} = 175.6 Hz (t), CH₂).

4. Spectroscopic properties of oxirane

Oxirane, c -C₂H₄O, is a very asymmetric rotor of the oblate type with $\kappa = (2B - A - C)/(A - C) = 0.4093$. It has C_{2v} symmetry, and the b -axis is the symmetry axis, which is determined by the O atom and the mid-point of the CC bond, see also Fig. 2. The four equivalent H atoms lead to *para* and *ortho* spin-statistics. The a -axis is parallel to the CC bond, and the c -axis is perpendicular to the plane formed by the two C atoms and the O atom. The molecule possesses a sizable b -dipole moment of 1.90 D [11]; this value is 0.02 D larger than the originally reported one [7] because of updated values for the dipole moment of the OCS molecule [45, 46].

Substitution of one of the four H atoms by D lowers the symmetry to C_1 and leads to a chiral species. The rotation of the inertial axes with respect to those of the main isotopolog introduces a small a -dipole moment component of 0.36 D and a very small c -component of 0.08 D, as calculated from the structure [15]. It is also an asymmetric rotor, but with $\kappa = +0.2042$ even further away from the oblate limit of +1. Non-trivial spin-statistics do not exist in the mono-deuterated oxirane.

Substitution of two of the four H atoms by D leads to three different isotopomers, one with the two D on the

same C atom and two with one D on each C atom, either essentially opposite to each other or close to each other. The first one, oxirane-2,2- d_2 , is an asymmetric type rotor with $\kappa = +0.0229$ further away from the oblate limit still. The molecular symmetry is C_s , and it has a calculated a -dipole moment component of 0.50 D and a b -component of 1.81 D. No non-trivial spin-statistics are found in this doubly-deuterated oxirane. The second one is oxirane-*anti*-2,3- d_2 with C_2 symmetry, $\kappa = +0.0838$, only a b -dipole moment component, and *para* and *ortho* spin-statistics exist in this isotopomer. The third one is oxirane-*syn*-2,3- d_2 with C_s symmetry and $\kappa = +0.1280$. It possesses a very small c -dipole moment component besides an almost unchanged b -component. Non-trivial spin-statistics do not occur in this isotopomer. Hence, the three doubly deuterated oxirane isotopomers possess different molecular symmetries, which also differ from those of the mono- and undeuterated isotopologs. Please note that our designations of the doubly deuterated oxiranes in [15] were incorrect because atom 1 is the heteroatom, O in the present case, and that E and Z refer to planar configurations.

5. Analysis of the c -CD₂CH₂O rotational spectrum and determination of spectroscopic parameters

We used Pickett’s SPFIT and SPCAT programs [47] to fit and to calculate transition frequencies of oxirane-2,2- d_2 . In the absence of experimental data, we carried out quantum-chemical calculations at the Regionales Rechenzentrum der Universität zu Köln (RRZK) using the commercially available program Gaussian 09 [48]. We performed B3LYP hybrid density functional calculations [49, 50], utilizing the aug-cc-pVTZ (abbreviated aVTZ) basis set [51] to evaluate ground state rotational and quartic and sextic equilibrium distortion parameters of c -CD₂CH₂O, c -C₂H₃DO, and c -C₂H₄O in the S reduction and in the III’ representation. The results of the last two calculations and the corresponding experimental values of c -C₂H₃DO [15] and c -C₂H₄O [11] were taken to estimate correction factors to be applied to the calculated spectroscopic parameters of c -CD₂CH₂O in order to reduce short-comings of the quantum-chemical method and those caused by the differences between equilibrium and ground state distortion parameters as was done, e.g., for c -H₂C₃O [52].

The most easily recognizable patterns in the rotational spectrum of c -CD₂CH₂O are nearly oblate paired transitions as shown in Fig. 1. These are transitions with equal J and equal K_c and with K_c approaching J , which display small, but resolved asymmetry splitting.

The non-zero a -dipole moment component leads to two weaker transitions between the stronger b -type transitions. The respective R -branch transitions ($\Delta J = +1$) are among the strong transitions in the spectrum, in particular in the submillimeter region. Even stronger are oblate paired transition, where the asymmetry splitting is not resolved anymore, and prolate paired R -branch transitions, with equal J and equal K_a and with K_a approaching J . Since $\mu_c = 0$ in c -CD₂CH₂O, there are no accompanying c -type transitions for nearly prolate paired transitions, in contrast to c -C₂H₃DO, which possesses a very small c -dipole moment component.

All transitions in the 490–750 GHz range assigned in the first round were calculated somewhat higher than observed, and the deviations increased usually with J . This made the nearly oblate paired transitions with $J - K_c = 5$, of which the second group in this frequency range is shown in Fig. 1, particularly easy to identify because of the relatively small asymmetry splittings and the proximity to the calculated positions. The calculations were higher by ~ 35 MHz for the quartet of lines near 514.6 GHz and 114 MHz for the single line near 717.2 GHz. The deviations were larger for transitions with higher K_c , reaching more than 210 MHz for the unsplit $J = K_c = 28 - 27$ transitions near 719.5 GHz. Furthermore, the scatter in the deviations within the four line pattern increased to several tens of megahertz in the case of asymmetry splittings of several gigahertz. The 177 different lines, corresponding to 244 transitions because of unresolved asymmetry splitting, were fit with their uncertainties on average by employing rotational, quartic, and three sextic distortion parameters; these were H_K , H_{KJ} , and h_2 ; h_1 was kept fixed to its estimated value, whereas H_{JK} , H_J , and h_3 were omitted because neither was determinable with significance at this point, and in each case the omission of the parameter improved the quality of the fit compared to keeping it fixed to the initially estimated value. We point out that the oblate paired transitions were represented in the line lists only by the two strong b -type transitions. Adding the weaker a -type transitions to the list would only inflate the line list, but would have no effect on the parameter values or their uncertainties.

In the subsequent assignment rounds, lines with decreasing intensities were assigned. These included in the second round a -type transitions with higher K_a , b -type Q -branch transitions ($\Delta J = 0$), higher K_a transitions with $\Delta J = \Delta K_c = -\Delta K_a = +1$ (P -branch transitions), and b -type transitions with $\Delta K_a = 3$. Later assignments include several a -type transitions with $\Delta K_a = +2$. Eventually, the line list from this frequency region consisted of 987 different lines, corresponding to 1362

Table 1: Spectroscopic parameters^a (MHz) of oxirane-2,2-*d*₂ using Watson’s S reduction of the rotational Hamiltonian in the oblate representation III^l and in the prolate representation I^r along with the dimensionless weighted standard deviation wrms.

Parameter	III ^l			I ^r
	Experimental	B3LYP/aVTZ ^b	Scaled ^c	Experimental
<i>A</i>	23062.786666 (35)	23018.956	23066.253	23062.777841 (35)
<i>B</i>	18013.451323 (29)	17925.922	18013.056	18013.452264 (29)
<i>C</i>	12727.735907 (32)	12663.953	12727.519	12727.743322 (32)
<i>D</i> _{<i>K</i>} × 10 ³	10.18394 (7)	10.117	10.117	12.53427 (13)
<i>D</i> _{<i>JK</i>} × 10 ³	−36.85961 (12)	−36.652	−39.767	25.30088 (14)
<i>D</i> _{<i>J</i>} × 10 ³	33.52691 (8)	33.286	33.852	12.33667 (6)
<i>d</i> ₁ × 10 ³	7.395157 (30)	7.3566	7.9437	−3.435028 (17)
<i>d</i> ₂ × 10 ³	−0.927347 (11)	−0.940	−1.0172	−0.692299 (7)
<i>H</i> _{<i>K</i>} × 10 ⁹	−36.618 (67)	−20.28	−20.28	6.023 (181)
<i>H</i> _{<i>KJ</i>} × 10 ⁹	64.224 (160)	37.57	37.57	125.017 (310)
<i>H</i> _{<i>JK</i>} × 10 ⁹	−40.398 (164)	−53.7	−80.5	−92.878 (194)
<i>H</i> _{<i>J</i>} × 10 ⁹	15.556 (75)	36.6	36.6	14.799 (48)
<i>h</i> ₁ × 10 ⁹	−7.585 (35)	−14.2	−1.42	4.109 (14)
<i>h</i> ₂ × 10 ⁹	11.005 (19)	5.56	6.67	−1.169 (8)
<i>h</i> ₃ × 10 ⁹	−0.119 (4)	−2.07	2.11	0.739 (2)
<i>L</i> _{<i>K</i>} × 10 ¹²	−0.359 (25)			−3.628 (133)
<i>L</i> _{<i>KKJ</i>} × 10 ¹²	1.041 (72)			1.624 (246)
<i>L</i> _{<i>JK</i>} × 10 ¹²	−1.381 (92)			2.033 (188)
<i>L</i> _{<i>JJK</i>} × 10 ¹²	1.261 (61)			−1.841 (81)
<i>L</i> _{<i>J</i>} × 10 ¹²	−0.561 (21)			0.070 (14)
<i>l</i> ₁ × 10 ¹⁵	284.4 (116)			−26.9 (37)
<i>l</i> ₂ × 10 ¹⁵	−160.7 (75)			−58.0 (28)
<i>l</i> ₃ × 10 ¹⁵	127.1 (24)			2.37 (79)
<i>l</i> ₄ × 10 ¹⁵	−18.8 (7)			−1.05 (13)
wrms	0.794			0.794

^aNumbers in parentheses are one standard deviation in units of the least significant figures.

^bGround state rotational and equilibrium quartic and sextic centrifugal distortion parameters calculated employing B3LYP/aug-cc-pVTZ.

^cB3LYP/aug-cc-pVTZ spectroscopic parameters scaled with ratios determined from experimental and quantum-chemically calculated values from *c*-C₂H₃DO and *c*-C₂H₄O.

Table 2: Spectroscopic parameters^a (MHz) of oxirane-2,2-*d*₂ using Watson’s A reduction of the rotational Hamiltonian in the oblate representation III^l and in the prolate representation I’ along with the dimensionless weighted standard deviation wrms.

Parameter	III ^l	I’
<i>A</i>	23062.767432 (35)	23062.770912 (35)
<i>B</i>	18013.477996 (29)	18013.471157 (29)
<i>C</i>	12727.726637 (32)	12727.729962 (32)
$\Delta_K \times 10^3$	19.45745 (12)	19.45707 (11)
$\Delta_{JK} \times 10^3$	47.98798 (17)	16.99339 (11)
$\Delta_J \times 10^6$	35.38168 (8)	13.72127 (6)
$\delta_K \times 10^3$	11.47547 (14)	8.06040 (8)
$\delta_J \times 10^3$	7.39502 (3)	3.43503 (2)
$\Phi_K \times 10^9$	−50.52 (45)	86.32 (14)
$\Phi_{KJ} \times 10^9$	194.09 (70)	−1.26 (20)
$\Phi_{JK} \times 10^9$	−178.44 (34)	−44.54 (13)
$\Phi_J \times 10^9$	37.60 (8)	12.47 (5)
$\phi_K \times 10^9$	−1.55 (43)	81.13 (8)
$\phi_{JK} \times 10^9$	129.59 (25)	−18.36 (9)
$\phi_J \times 10^9$	−7.70 (4)	4.864 (13)
$L_K \times 10^{12}$	−22.31 (82)	−5.20 (14)
$L_{KKJ} \times 10^{12}$	51.13 (148)	4.43 (14)
$L_{JK} \times 10^{12}$	−38.15 (83)	
$L_{JJK} \times 10^{12}$	10.26 (20)	−2.48 (14)
$L_J \times 10^{12}$	−0.93 (3)	−0.055 (14)
$l_K \times 10^{12}$	−17.76 (65)	−0.83 (10)
$l_{KJ} \times 10^{12}$	18.08 (37)	
$l_{JK} \times 10^{12}$	−4.17 (12)	−0.59 (3)
$l_J \times 10^{12}$	0.411 (12)	−0.030 (4)
wrms	0.801	0.799

^aNumbers in parentheses are one standard deviation in units of the least significant figures.

transitions. These were fit with a full set of distortion parameters up to eighth order with all of them significantly determined, albeit L_J just barely.

We point out that, even though our sample of *c*-CD₂CH₂O contained substantial amounts of *c*-C₂H₃DO and even some *c*-C₂H₄O, line blending with other isotopic species or with excited vibrational states appeared to be only slightly more important than in our investigation of *c*-C₂H₃DO [15] for the most part, except probably for the very weak lines which appeared to be more affected by line blending in the present study.

The 490–750 GHz region was also recorded in its entirety in our investigation of *c*-C₂H₃DO [15]. Therefore, we checked these recordings for the presence of oxirane-2,2-*d*₂ in that sample. We identified lines easily, albeit at a level of only ~0.1%, which is only a modest level of enrichment compared to the ~0.015% expected because of the naturally occurring deuterium.

Subsequently, we added transitions recorded around 1 THz. These were 103 strong or very strong transitions and 52 weak transitions with high K_a or very weak transitions with high K_c . Many of the intended high K_c transitions were too weak, heavily blended, or too close to neighboring lines such that only few of them were added to the line list. In the case of the intended high K_a transitions, a smaller fraction of the lines was not used. Most of these lines correspond to unresolved asymmetry doublets, the number of different lines from this frequency region is 85. The uncertainties of all spectroscopic parameters were smaller after inclusion of these lines, most notably L_J because of the strong or very strong lines with K_c close to or equal to J .

Finally, we included 178 stronger and 39 weaker transitions from the 120–181 GHz region to the line list. Each of them corresponds to a single transition. The parameter uncertainties improved somewhat as a consequence.

These data add up to 1289 different transition frequencies and 1734 transitions. The J quantum numbers range from 2 to 58 with $K_a \leq 42$ and $K_c \leq 53$. After having determined the final line list and the final set of spectroscopic parameters in the S reduction and the III^l representation, we also evaluated parameters applying the A reduction and the S and A reductions in the I’ representation. The experimental S reduction parameters are presented in Table 1 together with quantum-chemically calculated and scaled values in the III^l representation; the experimental A reduction values are given in Table 2. The weighted standard deviations for each fit are also included in the tables. We also determined the weighted standard deviations of the lines from each assignment round. These values were between 0.64 and

0.97, mostly closer to the value of the entire fit. We also mention that the rms values for the four fits are all very close to 12 kHz. The rms value of a fit is a meaningful measure of the quality of the fit if the uncertainties of the lines differ very little. There is an uncertainty scatter in the present line list such that the rms value is dominated by the lines with larger uncertainties. Nevertheless, the rms values provide an indication of the average quality of the lines.

The final c -CD₂CH₂O line file, the parameter and fit files in the S reduction and the III^l representation are available as supplementary material to this article. The line file and all parameter and fit files along with auxiliary files are provided in the data section¹ of the Cologne Database for Molecular Spectroscopy, CDMS [53, 54]. A calculation of the rotational spectrum of c -CD₂CH₂O based on the fit in the S reduction and the III^l representation is available in the CDMS catalog².

6. Discussion of the laboratory results

The c -CD₂CH₂O parameter set in the S reduction and the III^l representation is very similar in extent and absolute uncertainties to those of c -C₂H₃DO [15] and c -C₂H₄O [11]. Therefore, the data should be sufficiently accurate for all radio astronomical observations.

It is noteworthy that the A reduction in the III^l representation yields a fit of essentially identical quality with the same number of spectroscopic parameters. This is in sharp contrast to c -C₂H₄O, for which a fit employing this combination of reduction and representation gave a still poor fit with a much larger parameter set. We carried out a corresponding fit for c -C₂H₃DO in order to gain more insight into the performance of the A reduction in the III^l representation. It turned out that the same set of parameters as the A reduction in the I^r representation yielded a fit with only slightly larger weighted rms error. This fit and a fit using the S reduction in the I^r representation are available in the data section¹ of the CDMS [53, 54]. The poor performance of the A reduction in an oblate representation is quite common, see [11] for several examples, but apparently not ubiquitous. Rotational spectra of molecules closer to the oblate limit are obviously more likely to yield poor fits, but $\kappa = 0.4093$ in the case of c -C₂H₄O is quite far from the oblate limit of +1, suggesting other aspects matter as well, which could, for example, be the quantum number range or the extent to which asymmetry plays a role in the experimental line list.

¹<https://cdms.astro.uni-koeln.de/classic/predictions/daten/Oxiran/>

²<https://cdms.astro.uni-koeln.de/classic/entries/>

The rotational and quartic centrifugal distortion parameters from a quantum-chemical calculation agree quite well after scaling with the experimental ones, as can be seen in Table 1, but the agreement is less good for the sextic distortion parameters and in some case, the unscaled values are closer to the experimental values of the quartic and sextic distortion parameters. A similar procedure was applied to the spectroscopic parameters up to sixth order of c -C₂H₃DO using higher level coupled cluster calculations [55]. The sextic distortion parameters agree somewhat better with the experimental ones [15] than in the present case of c -CD₂CH₂O, but the quality differences are less pronounced for the lower order parameters. This demonstrates that lower level calculations, such as B3LYP, can be an alternative to coupled cluster calculations which can get quite demanding in terms of time and memory for larger molecules.

7. Astronomical search toward IRAS 16293-2422 B

We used the calculation of the rotational spectrum of c -CD₂CH₂O as described at the end of Section 5 to search for this isotopolog in data from PILS. As mentioned in the introduction, PILS is an unbiased molecular line survey of the protostellar object IRAS 16293–2422 carried out with ALMA in its Cycle 2 (project id: 2013.1.00278.S, PI: J. K. Jørgensen). The source is separated into two main components, the more prominent Source A, which itself is a binary source [56], and the secondary Source B, separated by about 5 arcsec (700 au); both are commonly viewed as Class 0 protostars. The survey covers part of Band 7 from 329.1 to 362.9 GHz at 0.2 km s⁻¹ spectral and ~0.5 arcsec angular resolution. Jørgensen et al. provides an overview of the data and their reduction along with first results from the survey [16].

For the search for c -CD₂CH₂O, we focus on a position offset by one beam from source B, also targeted in several previous studies of the molecular complexity in PILS (e.g., [16, 20, 27]). This position is ideal because of the narrow lines seen there (~1 km s⁻¹), which allows for searches for rare species and limited continuum opacity causing absorption to be less severe. We performed the search by fitting synthetic spectra for c -CD₂CH₂O to the ALMA data. The synthetic spectra are calculated under the assumption of the emission being optically thin and the excitation being in local thermodynamical equilibrium. This is a valid assumption given the high densities in the molecular cloud surrounding the protostar that is probed by our ALMA observations [16]. We assumed $T_{\text{rot}} = 125$ K in our initial

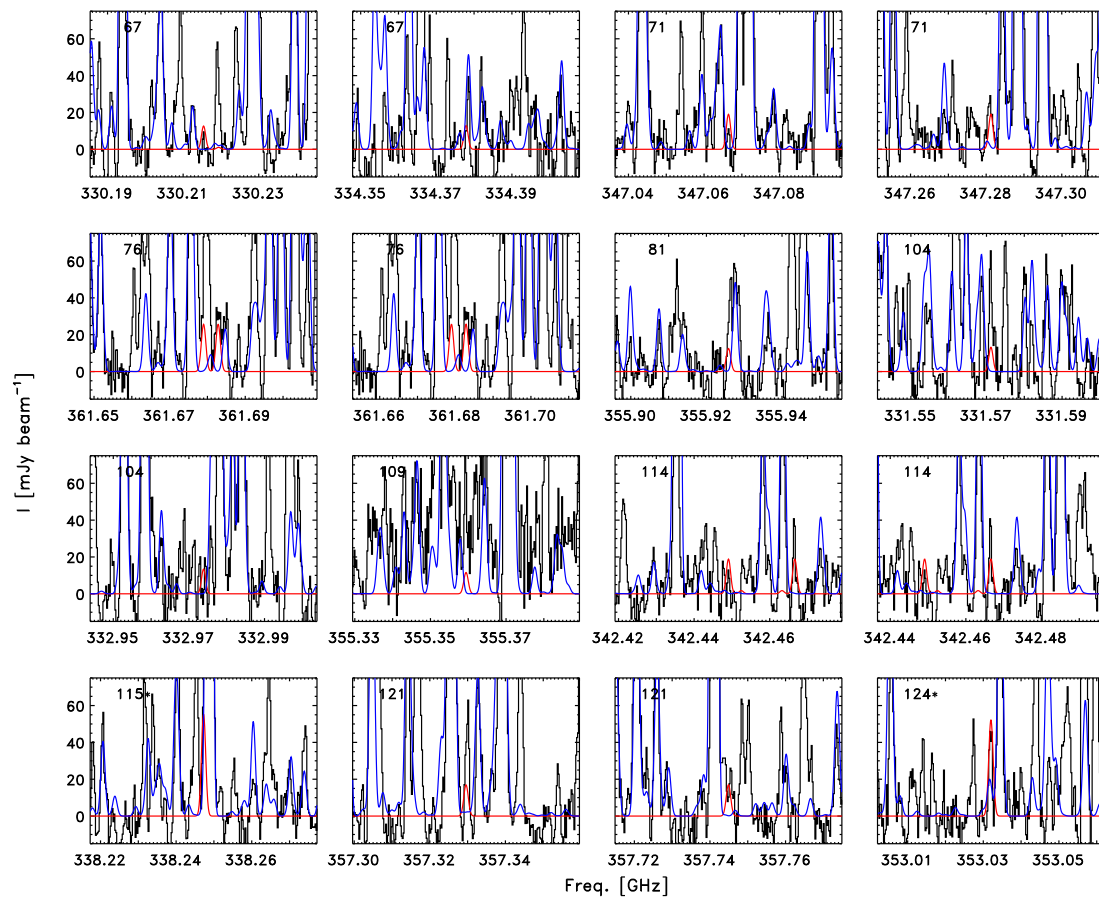


Figure 3: Sections of the Band 7 PILS data slightly offset from the continuum peak displaying stronger lines of $c\text{-CH}_2\text{CD}_2\text{O}$. The observed data are shown in black, the modeled $c\text{-CH}_2\text{CD}_2\text{O}$ lines in red, and the models of all other assigned lines in blue. The upper state energy of each line is given in the upper left corner of each panel.

Table 3: Sixteen emission lines (GHz) predicted to be the brightest in the PILES frequency range with quantum numbers QN, upper state energy, E_{up} (K), Einstein A value (10^{-4} s^{-1}), and line strength W (mJy km s^{-1}).

Frequency	QN	E_{up}	A	W
330.2154	$8_{6,3} - 7_{5,2}$	67	3.52	15.8
331.5712	$11_{3,8} - 10_{4,7}$	104	3.65	16.5
332.9739	$11_{4,8} - 10_{3,7}$	104	3.71	16.8
334.3779	$8_{6,2} - 7_{5,3}$	67	3.59	16.1
338.2473	$13_{x,13} - 12_{x,12}^a$	115	14.52	32.0
342.4491	$12_{2,10} - 11_{3,9}$	114	5.23	23.6
342.4666	$12_{3,10} - 11_{2,9}$	114	5.23	23.6
347.0665	$8_{7,2} - 7_{6,1}$	71	5.49	23.8
347.2813	$8_{7,1} - 7_{6,2}$	71	5.50	23.8
353.0320	$13_{x,12} - 12_{x,11}^b$	124	14.72	30.2
355.3594	$11_{5,7} - 10_{4,6}$	109	3.33	14.5
355.9258	$9_{6,4} - 8_{5,3}$	81	3.48	15.7
357.3296	$12_{3,9} - 11_{4,8}$	121	4.94	21.2
357.7449	$12_{4,9} - 11_{3,8}$	121	4.96	21.3
361.6790	$8_{8,1} - 7_{7,0}$	76	7.73	32.1
361.6828	$8_{8,0} - 7_{7,1}$	76	7.73	32.1

^aBlend of the oblate paired $13_{0,13} - 12_{1,12}$ and $13_{1,13} - 12_{0,12}$ transitions (additional minor contributions from the corresponding *a*-type transitions). ^bBlend of the oblate paired $13_{1,13} - 12_{2,12}$ and $13_{2,13} - 12_{1,12}$ transitions (additional minor contributions from the corresponding *a*-type transitions).

calculations as was determined for *c*-C₂H₄O [5] and employed a linewidth (FWHM) of 1 km s^{-1} and a velocity offset relative to the local standard of rest of 2.6 km s^{-1} , similar to other species toward this position.

Fig. 3 shows the 16 emission lines predicted to be brightest for the assumed value of T_{rot} . These represent 18 rotational transitions but where two sets of two transitions, respectively, are so close in frequency that they cannot be separated in the observations. The transitions, their frequencies, energies of their upper levels above the ground state and predicted strengths assuming the maximum possible column density are summarized in Table 3. For some of these predicted lines, no clear signal is seen down to the RMS noise level of the data (1σ being $4\text{--}5 \text{ mJy beam}^{-1} \text{ km s}^{-1}$), but a handful of predicted lines are seen to match observed features with line strengths above $20 \text{ mJy beam}^{-1} \text{ km s}^{-1}$. Importantly, if the column density is constrained based on these transitions, no lines are predicted to be significant where no observed emission is seen – an important criterion for the assignment of species in astronomical spectra.

Another test of the possible assignment can be taken from the derived column density from the tentative lines: the line strengths of those imply a column density of $3.3 \times 10^{14} \text{ cm}^{-2}$. This value can be compared to the column density of the mono-deuterated variant for the same T_{rot} of $8.9 \times 10^{14} \text{ cm}^{-2}$ [15], corresponding to a ratio of the doubly to mono-deuterated variants of 0.37. Taking $6.1 \times 10^{15} \text{ cm}^{-2}$ for *c*-C₂H₄O [5], we obtain a respective ratio of 0.054. Considering that there are statistically two ways to form *c*-CD₂CH₂O, but only one for *c*-C₂H₄O, this gives a D/H ratio of $\sim 16\%$ per H atom. This would, in turn, correspond to an enhancement by factor of 4.5 compared to the ~ 0.036 per H atom obtained from the ratio between *c*-C₂H₃DO and the non-deuterated variant *c*-C₂H₄O. This enhancement is similar to enhancement of other di-deuterated variants observed toward IRAS 16293-2422 B including CHD₂CN [27], CHD₂OCHO [28], CH₃OCHD₂ [29], CHD₂OH [30], and CHD₂CHO [57], and the inferred D/H ratios falls to those in the range of approximately 15–25%. This points to a common formation mechanism of these species including efficient H-D substitution reactions on grain-surfaces at low temperatures with these being more efficient one the first deuteration has occurred, see discussion in [30].

Still, our astronomical results on *c*-CD₂CH₂O should be viewed with some caution as the number of identified lines is on the low side to claim a definitive detection. One way to solidify the results lies in the detection of the other two doubly deuterated isotopomers of ox-

rane. All H atoms in *c*-C₂H₄O are chemically equivalent even if the three doubly deuterated isotopomers display different molecular symmetries. We expect in particular that all doubly deuterated isotopomers display the same degree of deuterium enrichment. Thus, characterizations of those would make it possible to verify the assignment of *c*-CD₂CH₂O and the interpretation that it indeed shows equivalent properties in terms of the deuterium enhancement as the other complex organics mentioned above.

8. Conclusion

We prepared a sample of oxirane-2,2-*d*₂, *c*-CD₂CH₂O, and analyzed its rotational spectrum for the first time. The resulting extensive set of spectroscopic parameters is accurate enough to search for this isotopolog in space. Using PLS data of IRAS 16293–2422, we tentatively identified a handful of lines of this isotopolog toward source B: with a column density derived on basis of these lines, no other non-detected features are predicted. The inferred column density of oxirane-2,2-*d*₂ would suggest an enhancement of this di-deuterated variant relative to the mono-deuterated variant similar to what has been observed for other complex organic molecules, an indication of their common formation of low temperatures. We suggest further characterizations and searches of the di-deuterated isotopomers of oxirane to verify these results.

CRedit authorship contribution statement

Holger S.P. Müller: Conceptualization, Investigation, Methodology, Formal analysis, Validation, Data curation, Writing – Original Draft, Writing – review & editing. Jes K. Jørgensen: Resources, Writing – Original Draft, Writing – review & editing. Jean-Claude Guillemin: Resources, Writing – Original Draft, Writing – review & editing. Frank Lewen: Resources, Writing – review & editing. Stephan Schlemmer: Funding acquisition, Resources, Writing – review & editing.

Declaration of competing interest

The authors declare that they have no known competing financial interests or personal relationships that could have appeared to influence the work reported in this paper.

Data availability

The spectroscopic line lists and associated files are available as supplementary material through the journal and in the data section of the CDMS.¹ The underlying original spectral recordings will be shared on reasonable request to the corresponding author. The radio astronomical data are available through the ALMA archive.³

Acknowledgments

We dedicate this work to the memories of Per Jensen and Helge Willner, two former professors at Bergische Universität Wuppertal, Germany, who recently passed away. This paper makes use of the following ALMA data: ADS/JAO.ALMA#2013.1.00278.S. ALMA is a partnership of ESO (representing its member states), NSF (USA) and NINS (Japan), together with NRC (Canada), NSC and ASIAA (Taiwan) and KASI (Republic of Korea), in cooperation with the Republic of Chile. The Joint ALMA Observatory is operated by ESO, AUI/NRAO and NAOJ. The work in Köln was supported by the Deutsche Forschungsgemeinschaft through the collaborative research center SFB 956 (project ID 184018867) project B3 and through the Gerätezentrum SCHL 341/15-1 (“Cologne Center for Terahertz Spectroscopy”). We thank the Regionales Rechenzentrum der Universität zu Köln (RRZK) for providing computing time on the DFG funded High Performance Computing System CHEOPS. J.K.J. acknowledges support from the Independent Research Fund Denmark (grant number 0135-00123B). J.-C. G. acknowledges support by the Centre National d’Etudes Spatiales (CNES; grant number 4500065585) and by the Programme National Physique et Chimie du Milieu Interstellaire (PCMI) of CNRS/INSU with INC/INP co-funded by CEA and CNES. Our research benefited from NASA’s Astrophysics Data System (ADS).

Appendix A. Supplementary Material

Supplementary data associated with this article can be found, in the online version, at <https://doi.org/10.1016/j.jms.2023.111777>. This material consists of fit, line, and parameter files along with an explanatory file. All files are ascii text files which are gathered in a zip file.

³<https://almascience.eso.org/aq/>

References

- [1] J. E. Dickens, W. M. Irvine, M. Ohishi, M. Ikeda, S. Ishikawa, A. Nummelin, Å. Hjalmarson, Detection of Interstellar Ethylene Oxide ($c\text{-C}_2\text{H}_4\text{O}$), *Astrophys. J.* 489 (1997) 753–757. doi:10.1086/304821.
- [2] A. Nummelin, J. E. Dickens, P. Bergman, A. Hjalmarson, W. M. Irvine, M. Ikeda, M. Ohishi, Abundances of ethylene oxide and acetaldehyde in hot molecular cloud cores, *Astron. Astrophys.* 337 (1998) 275–286.
- [3] M. Ikeda, M. Ohishi, A. Nummelin, J. E. Dickens, P. Bergman, Å. Hjalmarson, W. M. Irvine, Survey Observations of $c\text{-C}_2\text{H}_4\text{O}$ and CH_3CHO toward Massive Star-forming Regions, *Astrophys. J.* 560 (2001) 792–805. doi:10.1086/322957.
- [4] M. A. Requena-Torres, J. Martín-Pintado, S. Martín, M. R. Morris, The Galactic Center: The Largest Oxygen-bearing Organic Molecule Repository, *Astrophys. J.* 672 (2008) 352–360. arXiv:0709.0542, doi:10.1086/523627.
- [5] J. M. Lykke, A. Coutens, J. K. Jørgensen, M. H. D. van der Wiel, R. T. Garrod, H. S. P. Müller, P. Bjerkeli, T. L. Bourke, H. Calcutt, M. N. Drozdovskaya, C. Favre, E. C. Fayolle, S. K. Jacobsen, K. I. Öberg, M. V. Persson, E. F. van Dishoeck, S. F. Wampfler, The ALMA-PILS survey: First detections of ethylene oxide, acetone and propanal toward the low-mass protostar IRAS 16293-2422, *Astron. Astrophys.* 597 (2017) A53. arXiv:1611.07314, doi:10.1051/0004-6361/201629180.
- [6] A. Bacmann, A. Faure, J. Bertheaud, Cold and Yet Complex: Detection of Ethylene Oxide in a Prestellar Core, *ACS Earth Space Chem.* 3 (6) (2019) 1000–1013. doi:10.1021/acsearthspacechem.9b00072.
- [7] J. Cunningham, George L., A. W. Boyd, R. J. Myers, W. D. Gwinn, W. I. Le Van, The Microwave Spectra, Structure, and Dipole Moments of Ethylene Oxide and Ethylene Sulfide, *J. Chem. Phys.* 19 (6) (1951) 676–685. doi:10.1063/1.1748331.
- [8] C. Hirose, Laboratory Microwave Spectrum of Ethylene Oxide, *Astrophys. J. Lett.* 189 (1974) L145. doi:10.1086/181487.
- [9] J. Pan, S. Albert, K. V. L. N. Sastry, E. Herbst, F. C. De Lucia, The Millimeter- and Submillimeter-Wave Spectrum of Ethylene Oxide ($c\text{-C}_2\text{H}_4\text{O}$), *Astrophys. J.* 499 (1998) 517–519. doi:10.1086/305638.
- [10] C. Medcraft, C. D. Thompson, E. G. Robertson, D. R. T. Apudoo, D. McNaughton, The Far-infrared Rotational Spectrum of Ethylene Oxide, *Astrophys. J.* 753 (2012) 18. doi:10.1088/0004-637X/753/1/18.
- [11] H. S. P. Müller, J.-C. Guillemin, F. Lewen, S. Schlemmer, Rotational spectroscopy of isotopic oxirane, $c\text{-C}_2\text{H}_4\text{O}$, *J. Mol. Spectrosc.* 384 (2022) 111584. arXiv:2201.09266, doi:10.1016/j.jms.2022.111584.
- [12] C. Hirose, Microwave-spectra and r_0 , r_s , and r_m structures of ethylene-oxide, *Bull. Chem. Soc. Japan* 47 (6) (1974) 1311–1318. doi:10.1246/bcsj.47.1311.
- [13] R. A. Creswell, R. H. Schwendeman, Centrifugal distortion and oxygen-17 quadrupole coupling in ethylene oxide, *Chem. Phys. Lett.* 27 (1974) 521–524. doi:10.1016/0009-2614(74)80295-2.
- [14] S. Albert, Z. Chen, K. Keppler, P. Lerch, M. Quack, V. Schurig, O. Trapp, The Gigahertz and Terahertz spectrum of monodeutero-oxirane ($c\text{-C}_2\text{H}_3\text{DO}$), *Phys. Chem. Chem. Phys.* 21 (2019) 3669–3675. doi:10.1039/C8CP05311A.
- [15] H. S. P. Müller, J. K. Jørgensen, J.-C. Guillemin, F. Lewen, S. Schlemmer, Rotational spectroscopy of mono-deuterated oxirane ($c\text{-C}_2\text{H}_3\text{DO}$) and its detection towards IRAS 16293-2422 B, *Mon. Not. R. Astron. Soc.* 518 (2023) 185–193. arXiv:2209.01414, doi:10.1093/mnras/stac2525.
- [16] J. K. Jørgensen, M. H. D. van der Wiel, A. Coutens, J. M. Lykke, H. S. P. Müller, E. F. van Dishoeck, H. Calcutt, P. Bjerkeli, T. L. Bourke, M. N. Drozdovskaya, C. Favre, E. C. Fayolle, R. T. Garrod, S. K. Jacobsen, K. I. Öberg, M. V. Persson, S. F. Wampfler, The ALMA Protostellar Interferometric Line Survey (PILS). First results from an unbiased submillimeter wavelength line survey of the Class 0 protostellar binary IRAS 16293-2422 with ALMA, *Astron. Astrophys.* 595 (2016) A117. arXiv:1607.08733, doi:10.1051/0004-6361/201628648.
- [17] E. C. Fayolle, K. I. Öberg, J. K. Jørgensen, K. Altwegg, H. Calcutt, H. S. P. Müller, M. Rubin, M. H. D. van der Wiel, P. Bjerkeli, T. L. Bourke, A. Coutens, E. F. van Dishoeck, M. N. Drozdovskaya, R. T. Garrod, N. F. W. Ligterink, M. V. Persson, S. F. Wampfler, Rosina Team, Protostellar and cometary detections of organohalogens, *Nat. Astron.* 1 (2017) 703–708. doi:10.1038/s41550-017-0237-7.
- [18] A. Coutens, N. F. W. Ligterink, J.-C. Loison, V. Wakelam, H. Calcutt, M. N. Drozdovskaya, J. K. Jørgensen, H. S. P. Müller, E. F. van Dishoeck, S. F. Wampfler, The ALMA-PILS survey: First detection of nitrous acid (HONO) in the interstellar medium, *Astron. Astrophys.* 623 (2019) L13. arXiv:1903.03378, doi:10.1051/0004-6361/201935040.
- [19] A. Coutens, J. C. Loison, A. Boulanger, E. Caux, H. S. P. Müller, V. Wakelam, S. Manigand, J. K. Jørgensen, The ALMA-PILS survey: First tentative detection of 3-hydroxypropanal (HOCHCHCHO) in the interstellar medium and chemical modeling of the $\text{C}_3\text{H}_4\text{O}_2$ isomers, *Astron. Astrophys.* 660 (2022) L6. arXiv:2203.14119, doi:10.1051/0004-6361/202243038.
- [20] J. K. Jørgensen, H. S. P. Müller, H. Calcutt, A. Coutens, M. N. Drozdovskaya, K. I. Öberg, M. V. Persson, V. Taquet, E. F. van Dishoeck, S. F. Wampfler, The ALMA-PILS survey: isotopic composition of oxygen-containing complex organic molecules toward IRAS 16293-2422B, *Astron. Astrophys.* 620 (2018) A170. arXiv:1808.08753, doi:10.1051/0004-6361/201731667.
- [21] T. J. Millar, A. Bennett, E. Herbst, Deuterium fractionation in dense interstellar clouds, *Astrophys. J.* 340 (1989) 906–920. doi:10.1086/167444.
- [22] A. Crapsi, P. Caselli, C. M. Walmsley, P. C. Myers, M. Tafalla, C. W. Lee, T. L. Bourke, Probing the Evolutionary Status of Starless Cores through N_2H^+ and N_2D^+ Observations, *Astrophys. J.* 619 (2005) 379–406. arXiv:astro-ph/0409529, doi:10.1086/426472.
- [23] C. Ceccarelli, P. Caselli, E. Herbst, A. G. G. M. Tielens, E. Caux, Extreme Deuteration and Hot Corinos: The Earliest Chemical Signatures of Low-Mass Star Formation, Protostars and Planets V (2007) 47–62. arXiv:astro-ph/0603018.
- [24] V. Taquet, S. B. Charnley, O. Sipilä, Multilayer Formation and Evaporation of Deuterated Ices in Prestellar and Protostellar Cores, *Astrophys. J.* 791 (1) (2014) 1. arXiv:1405.3268, doi:10.1088/0004-637X/791/1/1.
- [25] J. Chantzos, S. Spezzano, P. Caselli, A. Chacón-Tanarro, L. Biz-zocchi, O. Sipilä, B. M. Giuliano, A Study of the $c\text{-C}_3\text{HD}/c\text{-C}_3\text{H}_2$ Ratio in Low-mass Star-forming Regions, *Astrophys. J.* 863 (2018) 126. arXiv:1807.04663, doi:10.3847/1538-4357/aad2dc.
- [26] M. V. Persson, J. K. Jørgensen, H. S. P. Müller, A. Coutens, E. F. van Dishoeck, V. Taquet, H. Calcutt, M. H. D. van der Wiel, T. L. Bourke, S. F. Wampfler, The ALMA-PILS Survey: Formaldehyde deuteration in warm gas on small scales toward IRAS 16293-2422 B, *Astron. Astrophys.* 610 (2018) A54. arXiv:1711.05736, doi:10.1051/0004-6361/201731684.
- [27] H. Calcutt, J. K. Jørgensen, H. S. P. Müller, L. E. Kristensen, A. Coutens, T. L. Bourke, R. T. Garrod, M. V. Persson, M. H. D.

- van der Wiel, E. F. van Dishoeck, S. F. Wampfler, The ALMA-PILS survey: complex nitriles towards IRAS 16293-2422, *Astron. Astrophys.* 616 (2018) A90. [arXiv:1804.09210](#), doi: 10.1051/0004-6361/201732289.
- [28] S. Manigand, H. Calcutt, J. K. Jørgensen, V. Taquet, H. S. P. Müller, A. Coutens, S. F. Wampfler, N. F. W. Ligterink, M. N. Drozdovskaya, L. E. Kristensen, M. H. D. van der Wiel, T. L. Bourke, The ALMA-PILS survey: the first detection of doubly deuterated methyl formate (CHD₂OCHO) in the ISM, *Astron. Astrophys.* 623 (2019) A69. [arXiv:1811.09102](#), doi: 10.1051/0004-6361/201832844.
- [29] C. Richard, J. K. Jørgensen, L. Margulès, R. A. Motiyenko, J. C. Guillemin, P. Groner, Torsional-rotational spectrum of doubly deuterated dimethyl ether (CH₃OCHD₂). First ALMA detection in the interstellar medium, *Astron. Astrophys.* 651 (2021) A120. [arXiv:2106.07983](#), doi:10.1051/0004-6361/202141282.
- [30] M. N. Drozdovskaya, L. H. Coudert, L. Margulès, A. Coutens, J. K. Jørgensen, S. Manigand, Successive deuteration in low-mass star-forming regions: The case of D₂-methanol (CHD₂OH) in IRAS 16293-2422, *Astron. Astrophys.* 659 (2022) A69. [arXiv:2201.07268](#), doi:10.1051/0004-6361/202142863.
- [31] V. V. Ilyushin, H. S. P. Müller, J. K. Jørgensen, S. Bauerecker, C. Maul, Y. Bakhmat, E. A. Alekseev, O. Dorovskaya, S. Vlasenko, F. Lewen, S. Schlemmer, K. Berezkin, R. M. Lees, Rotational and rovibrational spectroscopy of CD₃OH with an account of CD₃OH toward IRAS 16293–2422, *Astron. Astrophys.* 658 (2022) A127. [arXiv:2111.09055](#), doi:10.1051/0004-6361/202142326.
- [32] C. Vastel, T. G. Phillips, C. Ceccarelli, J. Pearson, First Detection of Doubly Deuterated Hydrogen Sulfide, *Astrophys. J. Lett.* 593 (2) (2003) L97–L100. [arXiv:astro-ph/0307221](#), doi:10.1086/378261.
- [33] J. Harju, O. Sipilä, S. Brünken, S. Schlemmer, P. Caselli, M. Juvela, K. M. Menten, J. Stutzki, O. Asvany, T. Kamiński, Y. Okada, R. Higgins, Detection of Interstellar Ortho-D₂H⁺ with SOFIA, *Astrophys. J.* 840 (2) (2017) 63. [arXiv:1704.02526](#), doi:10.3847/1538-4357/aa6c69.
- [34] M. Melosso, L. Bizzocchi, O. Sipilä, B. M. Giuliano, L. Dore, F. Tamassia, M. A. Martin-Drumel, O. Pirali, E. Redaelli, P. Caselli, First detection of NHD and ND₂ in the interstellar medium. Amidon deuteration in IRAS 16293-2422, *Astron. Astrophys.* 641 (2020) A153. [arXiv:2007.07504](#), doi: 10.1051/0004-6361/202038490.
- [35] S. S. Jensen, J. K. Jørgensen, L. E. Kristensen, A. Coutens, E. F. van Dishoeck, K. Furuya, D. Harsono, M. V. Persson, ALMA observations of doubly deuterated water: inheritance of water from the prestellar environment, *Astron. Astrophys.* 650 (2021) A172. [arXiv:2104.13411](#), doi:10.1051/0004-6361/202140560.
- [36] S. Spezzano, O. Sipilä, P. Caselli, S. S. Jensen, S. Czakli, L. Bizzocchi, J. Chantzos, G. Esplugues, A. Fuente, F. Eisenhauer, H₂CS deuteration maps towards the pre-stellar core L1544, *Astron. Astrophys.* 661 (2022) A111. [arXiv:2203.08234](#), doi: 10.1051/0004-6361/202243073.
- [37] H. Hidaka, M. Watanabe, A. Kouchi, N. Watanabe, Reaction Routes in the CO-H₂CO-d_n-CH₃OH-d_m System Clarified from H(D) Exposure of Solid Formaldehyde at Low Temperatures, *Astrophys. J.* 702 (1) (2009) 291–300. doi:10.1088/0004-637X/702/1/291.
- [38] Z. Chen, S. Albert, K. Keppler, M. Quack, V. Schurig, O. Trapp, High-resolution gigahertz and terahertz spectroscopy of the isotopically chiral molecule trans-2,3-dideutero-oxirane (*c*-CHD-CHDO), in: 2021 International Symposium on Molecular Spectroscopy, 2021. doi:10.15278/isms.2021.WJ01.
- [39] M. H. Ordu, H. S. P. Müller, A. Walters, M. Nuñez, F. Lewen, A. Belloche, K. M. Menten, S. Schlemmer, The quest for complex molecules in space: laboratory spectroscopy of *n*-butyl cyanide, *n*-C₄H₉CN, in the millimeter wave region and its astronomical search in Sagittarius B2(N), *Astron. Astrophys.* 541 (2012) A121. [arXiv:1204.2686](#), doi:10.1051/0004-6361/201118738.
- [40] L.-H. Xu, R. M. Lees, G. T. Crabbe, J. A. Myshrall, H. S. P. Müller, C. P. Endres, O. Baum, F. Lewen, S. Schlemmer, K. M. Menten, B. E. Billinghurst, Terahertz and far-infrared synchrotron spectroscopy and global modeling of methyl mercaptan, CH₃³²S, *J. Chem. Phys.* 137 (10) (2012) 104313–104313. doi:10.1063/1.4745792.
- [41] H. S. P. Müller, F. Lewen, Submillimeter spectroscopy of H₂C¹⁷O and a revisit of the rotational spectra of H₂C¹⁸O and H₂C¹⁶O, *J. Mol. Spectrosc.* 331 (2017) 28–33. [arXiv:1610.02174](#), doi:10.1016/j.jms.2016.10.004.
- [42] H. S. P. Müller, A. Belloche, F. Lewen, B. J. Drouin, K. Sung, R. T. Garrod, K. M. Menten, Toward a global model of the interactions in low-lying states of methyl cyanide: Rotational and rovibrational spectroscopy of the $\nu_4 = 1$ state and tentative interstellar detection of the $\nu_4 = \nu_8 = 1$ state in Sgr B2(N), *J. Mol. Spectrosc.* 378 (2021) 111449. [arXiv:2103.07389](#), doi:10.1016/j.jms.2021.111449.
- [43] H. S. P. Müller, O. Zingsheim, N. Wehres, J.-U. Grabow, F. Lewen, S. Schlemmer, Rotational Spectroscopy of the Lowest Energy Conformer of 2-Cyanobutane, *J. Phys. Chem. A* 121 (38) (2017) 7121–7129. doi:10.1021/acs.jpca.7b06072.
- [44] J.-C. Guillemin, W. Nasraoui, H. Gazzeh, Synthesis of N-unsubstituted cycloalkylimines containing a 4 to 8-membered ring, *Chem. Commun.* 55 (2019) 5647–5650.
- [45] K. Tanaka, T. Tanaka, I. Suzuki, Dipole moment function of carbonyl sulfide from analysis of precise dipole moments and infrared intensities, *J. Chem. Phys.* 82 (7) (1985) 2835–2844. doi:10.1063/1.448285.
- [46] J. G. Lahaye, R. Vandenhoute, A. Fayt, CO₂ laser saturation Stark spectra and global Stark analysis of carbonyl sulfide, *J. Mol. Spectrosc.* 119 (2) (1986) 267–279. doi:10.1016/0022-2852(86)90023-8.
- [47] H. M. Pickett, The fitting and prediction of vibration-rotation spectra with spin interactions, *J. Mol. Spectrosc.* 148 (2) (1991) 371–377. doi:10.1016/0022-2852(91)90393-0.
- [48] M. J. Frisch, G. W. Trucks, H. B. Schlegel, G. E. Scuseria, M. A. Robb, J. R. Cheeseman, G. Scalmani, V. Barone, B. Mennucci, G. A. Petersson, et al., Gaussian 09, Revision E.01, Gaussian, Inc., Wallingford CT (2013).
- [49] A. D. Becke, Density-functional thermochemistry. III. The role of exact exchange, *J. Chem. Phys.* 98 (7) (1993) 5648–5652. doi:10.1063/1.464913.
- [50] C. Lee, W. Yang, R. G. Parr, Development of the Colle-Salvetti correlation-energy formula into a functional of the electron density, *Phys. Rev. B* 37 (2) (1988) 785–789. doi:10.1103/PhysRevB.37.785.
- [51] T. H. Dunning, Jr., Gaussian basis sets for use in correlated molecular calculations. I. The atoms boron through neon and hydrogen, *J. Chem. Phys.* 90 (2) (1989) 1007–1023. doi: 10.1063/1.456153.
- [52] H. S. P. Müller, A. Brahmī M., J.-C. Guillemin, F. Lewen, S. Schlemmer, Rotational spectroscopy of isotopic cyclopropenone, *c*-H₂C₃O, and determination of its equilibrium structure, *Astron. Astrophys.* 647 (2021) A179. [arXiv:2102.03570](#), doi:10.1051/0004-6361/202040088.
- [53] H. S. P. Müller, F. Schlöder, J. Stutzki, G. Winnewisser, The

- Cologne Database for Molecular Spectroscopy, CDMS: a useful tool for astronomers and spectroscopists, *J. Mol. Struct.* 742 (1-3) (2005) 215–227. doi:10.1016/j.molstruc.2005.01.027.
- [54] C. P. Endres, S. Schlemmer, P. Schilke, J. Stutzki, H. S. P. Müller, The Cologne Database for Molecular Spectroscopy, CDMS, in the Virtual Atomic and Molecular Data Centre, VAMDC, *J. Mol. Spectrosc.* 327 (2016) 95–104. arXiv:1603.03264, doi:10.1016/j.jms.2016.03.005.
- [55] C. Puzzarini, M. Biczysko, J. Bloino, V. Barone, Accurate Spectroscopic Characterization of Oxirane: A Valuable Route to its Identification in Titan’s Atmosphere and the Assignment of Unidentified Infrared Bands, *Astrophys. J.* 785 (2) (2014) 107. doi:10.1088/0004-637X/785/2/107.
- [56] A. Wootten, The Duplicity of IRAS 16293-2422: A Protobinary Star?, *Astrophys. J.* 337 (1989) 858. doi:10.1086/167156.
- [57] J. Ferrer Asensio, S. Spezzano, L. H. Coudert, V. Lattanzi, C. P. Endres, J. K. Jørgensen, P. Caselli, Millimetre and sub-millimetre spectroscopy of doubly deuterated acetaldehyde (CHD₂CHO) and first detection towards IRAS 16293-2422, *Astron. Astrophys.* (2023) in press, arXiv:2301.06315, doi:10.1051/0004-6361/202245442.